machines

MDPI

Article

DenseNet-Enabled Intelligent Ship Energy Consumption Prediction Method with Navigation Information and Environmental Factors

Gulashan Tang [1,2], Rui Luo [3], Bin Huang [4], Xiang Li [3,*] and Hui Ma [1]

[1] Tsinghua Shenzhen International Graduate School, Shenzhen 518055, China
[2] Institute of Deep Sea Science and Engineering, Chinese Academy of Sciences, Sanya 572000, China
[3] Key Laboratory of Education Ministry for Modern Design and Rotor-Bearing System, Xi'an Jiaotong University, Xi'an 710049, China
[4] Hainan Moonsail Technology Co., Ltd., Sanya 572000, China
* Correspondence: lixiang@xjtu.edu.cn

Abstract: As a crucial procedure, ship energy consumption prediction is of great significance for the implementation of navigation planning, energy efficiency improvement, and emission reduction strategies. Currently, various studies have been conducted, primarily focusing on container ships, cargo ships, bulk carriers or tankers, with relatively fewer studies dedicated to research vessels. Regarding the limitations of low accuracy and poor effectiveness in ship energy consumption prediction, caused by the diverse voyages and specialized operational missions of research vessels, this paper proposes a DenseNet-enabled energy consumption prediction model considering the complex navigation information and diverse environmental factors. By leveraging the high parameter efficiency of DenseNet, effective feature extraction and strong generalization capabilities can be achieved, which provide more reliable and accurate predictions. Firstly, due to the fact that the real-time fuel consumption is influenced by a variety of internal and external factors, multi-source monitoring data are obtained and analyzed. After data analysis and feature extraction, the processed data and features are utilized to establish the prediction model. Through validations on the actual voyage data, it is demonstrated that the DenseNet-based prediction model outperforms the ResNet, DBCNN, and FCNN models in terms of both accuracy and predictive reliability. Therefore, the proposed method is capable of accurately predicting ship energy consumption under diverse shipping conditions and provides valuable guidance for the development of intelligent shipping.

Keywords: intelligent ship; energy consumption prediction; ship energy efficiency; deep learning; feature analysis

check for updates

Academic Editor: Farshid Naseri

Received: 9 December 2024
Revised: 10 January 2025
Accepted: 20 January 2025
Published: 22 January 2025

Citation: Tang, G.; Luo, R.; Huang, B.; Li, X.; Ma, H. DenseNet-Enabled Intelligent Ship Energy Consumption Prediction Method with Navigation Information and Environmental Factors. *Machines* **2025**, *13*, 76. https://doi.org/10.3390/machines13020076

Copyright: © 2025 by the authors. Licensee MDPI, Basel, Switzerland. This article is an open access article distributed under the terms and conditions of the Creative Commons Attribution (CC BY) license (https://creativecommons.org/licenses/by/4.0/).

1. Introduction

As one of the most important transportation modes over the world, though shipping brings great convenience to cargo transportation, it also causes a huge consumption of fossil fuels [1]. In accordance with the 4th International Maritime Organization (IMO) Greenhouse Gas (GHG) Research Report, the GHG emissions of total shipping has increased to 1.076 billion tonnes in 2018, accounting for 2.89% of the total anthropogenic CO_2 emissions worldwide [2,3]. Thus, several requirements and regulations were put forward by IMO to improve ship energy efficiency and reduce emissions, such as Energy Efficiency Design Index (EEDI) [4].

With the advancement of the modern maritime industry, the concept of intelligent shipping has emerged, which seeks to enhance operational efficiency and provide intelligent support for navigation safety [5]. As a critical indicator within the intelligent shipping, ship energy consumption not only indicates operating status of ship engines but also provides insights into the overall operating costs and exhaust emission levels [6]. Currently, predicting and optimizing ship energy consumption serves as an effective strategy to the ship intelligent energy efficiency management. As a fundamental step in this strategy, accurate energy consumption prediction plays a pivotal role in improving operational efficiency. Therefore, developing a reliable prediction method for ship energy consumption is crucial for reducing carbon emissions and enhancing overall efficiency.

So far, many scholars and industry practitioners have conducted research on ship energy consumption prediction and proposed some prediction and optimization methods. And ship energy consumption models can be generally classified to three categories: white-box model, black-box model and gray-box model [2,7].

White-box models are relatively common ship energy consumption models which are based on physical equations and empirical formulas between the internal and external parameters to establish the physical connection between the input and energy consumption of the ship system [8]. Islam et al. predicted the obstruction of container ships under different conditions through RaNS simulation, demonstrated that the optimum trim angle varies with ship speed and draft [9]. Yang et al. not only considers speed loss and speed correction but also takes the impact of ocean currents on ship speed and course into account [10]. Lu et al. proposed a semi-empirical model for predicting ship operational performance, which incorporates specific ship type deceleration factors and shape coefficients, thereby enhancing the accuracy of fuel consumption predictions for specific ships under different speeds, wave angles, drafts, and sea states. However, for long-distance voyages, the uncertainty of long-term weather forecasts may lead to large changes in the actual voyage route [11]. Wang et al. established a ship energy consumption prediction model that considers various navigational environmental factors, combining the analysis of the propeller and fuel consumption characteristics of the main engine [12]. However, white-box models are generally developed based on certain assumptions and simplifications during the modeling process, which may result in an incomplete consideration of feature variables [2]. Throughout a complete voyage, ship energy consumption is influenced by various internal and external factors, with navigation conditions being complex and variable. In such situations, relying on a white-box prediction model may lead to a large bias in the predicted results [13].

Black-box models, which are based on data analysis and constructed using statistical methods or machine learning techniques, without relying on the internal complex mechanism analysis of the system [14,15]. The prerequisite for accurate prediction is that black-box models can capture the underlying patterns in the data [16,17]. Zhou et al. developed a LASSO regression model for predicting ship fuel consumption, effectively integrating the impact of sea conditions and meteorological data, such as wind, waves, and currents, to enhance prediction accuracy. However, they neglected accidents and piracy, which might also affect the route planning [18]. Işıklı et al. employed the Response Surface Methodology (RSM) to establish a statistical model of ship fuel consumption based on the noon report data of a specific bulk carrier, which considered several determining factors affecting fuel consumption [19]. To avoid the inaccurate estimation of regression coefficients, Uyanık et al. established several prediction models for a container ship, such as Multiple Linear Regression model, Ridge and LASSO Regression model, Support Vector Regression model, and compared the accuracy of different models under the influence of various external factors [20]. Hu et al. proposed a two-step strategy for ship fuel consumption prediction and optimization, combining a hybrid model and trim adjustment to improve accuracy,

reduce fuel consumption, and cut carbon emissions. However, the rapid adjustment of a ship's trim still faces great challenges [21].

In recent years, with the rapid development of artificial intelligence technology and big data technology, data-based deep learning methods have also been applied in the field of ships. Farag et al. proposed a model which introduces Artificial Neural Network and Multiple Regression (MR) techniques to predict ship fuel consumption. The proposed model can operate in a real-time environment and adapt to possible changes in the ship's environment [22]. Yuan et al. developed a real-time fuel consumption prediction model based on Long Short-Term Memory (LSTM) Neural Network and adopted the Reduced Space Search Algorithm (RSSA) to optimize fuel consumption and overall voyage cost. Through optimization, the total fuel consumption is reduced by 33.54% and the total cost is reduced by 26.95% [23]. Chen et al. proposed a multi-step fuel consumption prediction model based on deep learning, utilizing the Ensemble Empirical Mode Decomposition-Long Short-Term Memory (EEMD-LSTM) network to improve accuracy, while employing the Bidirectional LSTM (BiLSTM) for short-term volatility prediction [24]. Prior studies have indicated that white-box models are generally more interpretable and need no data compared with black-box models [7,25]. However, black-box models can achieve high-precision prediction of ship energy consumption under complex environmental conditions when sufficient data are available [13,26]. In black-box models, the relationship between fuel consumption parameters is not explicitly defined in a formula but learned from the actual data [27,28].

Gray-box models are an effective combination of white-box and black-box models [2]. Based on data and mechanism analysis, they achieve a balance between good prediction accuracy and interpretability, while requiring comparatively less historical data [29]. Coraddu et al. proposed an innovative gray-box model with the ability to exploit both mechanistic knowledge and historical data, the proposed method can effectively reduce the ship fuel consumption [30]. To deal with the existing limitation of separating weather directions, Yang et al. combined gray-box model with genetic algorithm to estimate the unknown parameters; the established model achieved a good performance in ship fuel consumption prediction [31]. Although, gray-box models offer higher prediction accuracy and better interpretability, their performance not only depends on data quantity and quality but is also affected by the model's structure, assumptions, and incorporated physical laws [2,7,32].

Although many scholars have studied the energy consumption prediction of ships, the majority of studies still primarily focus on transport vessels such as cargo ships, container ships, bulk carriers and tankers, with relatively fewer studies dedicated to research vessels [2,7,33,34]. Additionally, trade routes between various ports for cargo transportation are generally fixed [35]. Due to the diverse and specialized operational missions of research vessel, the routes and voyage period generally vary, the navigation conditions, along with the marine environment and climatic factors they encounter, are significantly more complex [36,37]. This complexity poses challenges for existing research methods to achieve accurate energy consumption prediction for research vessels. To overcome the above challenges and enhance the energy efficiency management level of research vessels, this work collects various monitoring data of research vessel's voyage through multi-source sensors. Subsequently, specific data pre-processing and analysis would be performed in accordance with the actual operational conditions of the research vessel to extract the effective part. In the meantime, with the help of correlation analysis, the feature variables that have the highest correlation with ship energy consumption are screened out. The energy consumption prediction model is constructed based on the Densely Connected Convolutional Network (DenseNet), which would be verified by the processed data.

The remainder of this paper is organized as follows: Section 2 presents the problem formulation and modeling methods. Section 3 outlines the data processing and analysis techniques employed in this study. In Section 4, the energy consumption prediction model for the research vessel is developed and validated based on the analyzed data and extracted features. Section 5 concludes the paper and provides a discussion of the findings. Table 1 summarizes the models and their abbreviation used in the paper.

Table 1. A list of abbreviations.

Abbreviation	Explanation
RSSA	Reduced Space Searching Algorithm
LASSO	Least Absolute Shrinkage and Selection Operator
RSM	Response Surface Methodology
ResNet	Residual Network
FCNN	Fully Connected Neural Network
MR	Multiple Regression
LSTM	Long Short-Term Memory
DenseNet	Densely Connected Convolutional Network
CNN	Convolutional Neural Network
DBCNN	Deep Batch-Normalization Convolution Neural Network

2. Problem Formulation and Modeling Methods

2.1. Problem Formulation

The objective of energy consumption prediction is to accurately forecast the energy usage of research vessels under varying operational conditions and environmental factors. As global shipping increasingly prioritizes environmental sustainability and energy efficiency, reducing energy consumption has become vital for enhancing the economic performance of ships while minimizing the environmental impact. Therefore, developing an effective energy consumption prediction model for research vessels is essential for optimizing the vessel operation, route planning and fuel usage strategies.

The first step in this research involves identifying and extracting the critical feature variables that influence ship energy consumption. These factors may include parameters of navigation operational status and environmental factors, such as sailing speed, cargo load, wave height and wind speed. Then, these factors would be processed and serve as the input feature variables of the prediction model, enabling the model to capture the dynamic changes in energy consumption that occur under different scenarios. In addition, the energy consumption prediction values derived from different prediction models are supposed to be assessed through various evaluation metrics, such as Root Mean Square (RMSE) and the Coefficient of Determination (R^2), to ensure the reliability and accuracy of predictions across diverse operational scenarios.

2.2. Densely Connected Convolutional Network

Convolutional neural networks (CNNs) are a class of deep learning architectures that excel at processing structured grid data and highly nonlinear signals [38,39]. In recent years, numerous studies have achieved remarkable success in various applications, including image recognition, object detection, and fault diagnosis. CNNs utilize convolutional layers that apply filters to the input data, extracting the representative features in a hierarchical manner [7]. The architecture typically comprises convolutional layers, activation functions, pooling layers for down-sampling, and fully connected layers for classification. By capturing local patterns and reducing dimensionality through sparse connection and parameter weight sharing mechanism, CNNs effectively reduce the number of parameters, enhancing computational efficiency and generalization. Given that the input data in this study

combines processed navigation data and navigational environment data, one-dimensional convolution will be employed in the model.

However, in deep neural networks, the complexity of gradient computation increases the risk of vanishing and exploding gradients as the number of layers grows. The Residual Network (ResNet), first proposed in 2015, incorporates skip connection that allow data to flow directly from one layer to subsequent layers [40]. This design facilitates the flow of gradients during backpropagation, enabling ResNet to maintain performance and improve convergence rates. Consequently, it allows for the construction of much deeper networks without a significant increase in training complexity. Many research works have been inspired by this design [41–46].

The DenseNet, as an extension of ResNet, is designed to improve the flow of information and gradients throughout the network. Different from traditional architectures that connect each layer sequentially, DenseNet employs dense connectivity, where each layer is connected to all subsequent layers. This architecture promotes feature reuse, allowing each layer to access the features of all preceding layers, thus enhancing the network's efficiency and performance. Additionally, DenseNet introduces a growth rate parameter that regulates the number of features added at each layer, effectively balancing model complexity and capacity. The primary modules of DenseNet include: (1) dense block; (2) transition.

2.2.1. Dense Block

As illustrated in Figure 1, by adopting feature concatenation method, each layer in a dense block utilizes the information from all previous layers. Assuming that a dense block contains L layers, the number of connections in the block is $L * (L - 1)/2$. In a dense block, the output of the l-th layer is related to the outputs of all previous layers, which can be expressed as:

$$x^l = H^l([x^0, x^1, \ldots, x^{l-1}]) \quad (1)$$

where x^l denotes the output of l-th layer in the block, and $[x^0, x^1, \ldots, x^{l-1}]$ represents the concatenation process of the outputs from the previous $l - 1$ layers. $H^l(\bullet)$ represents the complex nonlinear transformation functions, which includes convolution, batch normalization (BN), and activation functions.

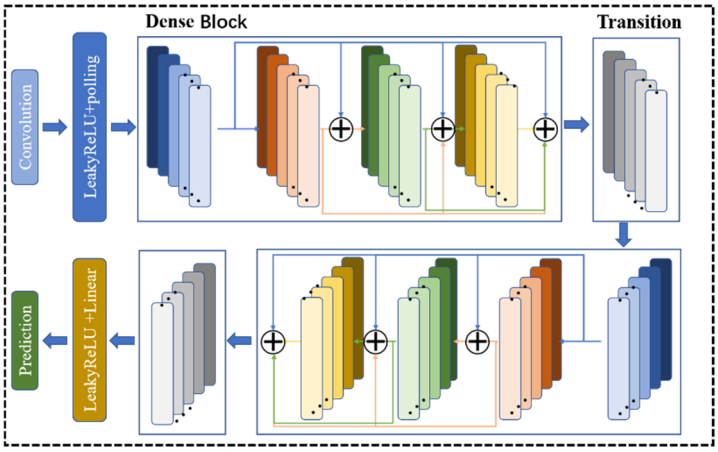


Figure 1. Densely connected convolutional network.

2.2.2. Transition

The transition module is positioned between two dense blocks and includes BN, convolution, and pooling operations. It is designed to reduce the number of features and lower their dimensionality while preserving essential information, which enhances the

efficiency and generalization ability of the prediction model. The detailed equations for these operations are expressed as follows:

$$\begin{aligned} n^{Tr} &= BN(x^L) \\ y^{Tr} &= \sigma(n^{Tr}) \\ x_l^{Tr} &= k_l^{Tr} * y^{Tr} + b_l^{Tr} \\ x_l^{Pool} &= maxpool(x_l^{Tr}, p, s) \end{aligned} \tag{2}$$

where x^L is the input to the transition module, σ represents the activation function, k_l^{Tr} and b_l^{Tr} denote the t-th convolutional kernel and bias parameter in the convolution operation. Additionally, *maxpool* refers to the max pooling operation, p and s represent the pooling size and stride, respectively, in the pooling operation. n^{Tr}, y^{Tr}, x^{Tr} and x^{pool} denote the outputs after the BN, activation function, convolution, and pooling operations in the transition module.

2.3. Overlap Sampling

Overlap sampling is a technique generally employed in time series data processing that involves extracting multiple samples from a continuous sequence of data through the usage of sliding windows. This method utilizes a sliding window mechanism defined by two critical parameters: the window size and the stride. Each sample consists of data points within the window, which can be used to compute features and corresponding target values. By increasing the effective sample size and capturing patterns within the data, overlap sampling can improve the robustness of models and ensure that the model can learn complex temporal dependencies.

$$x_{\text{input}}^t = \left(x_{\text{norm}}^{t-s+1}, \ldots, x_{\text{norm}}^{t-1}, x_{\text{norm}}^t \right) \tag{3}$$

where x_{input}^t represents the input sample data, x_{norm}^t represents the normalized data point at time t. The overlap sampling strategy leverages a time window of length s to concatenate the data obtained at consecutive s sampling moments into a high dimensional vector, which is used as the input to the prediction model. Accordingly, at the t-th sampling moment, the input to the prediction model not only contains the data obtained at the current moment but also includes the data from the previous $S-1$ moments. As shown in Figure 2, the window size and stride are set to 3 and 1, respectively. Therefore, at each sampling moment, the input to the prediction model will consist of monitoring data from 3 consecutive sampling moments.

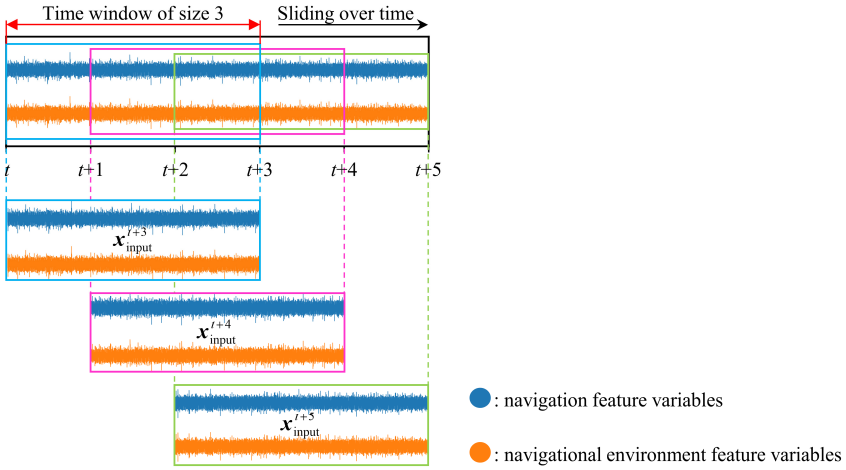


Figure 2. Overlap sampling illustration.

3. Multi-Source Data Analysis and Feature Extraction

3.1. Data Acquisition

To enhance the energy efficiency management level of the research vessel and achieve more accurate energy consumption prediction, several types of monitoring data need to be collected. These data can be broadly classified into two categories.

The first is navigation data, which encompasses both external factors, such as longitude and latitude of the navigation area, speed over ground (SOG), navigation trajectory, and course over ground (COG), as well as internal factors, including the fuel consumption rate, propeller speed, propeller direction, and propeller pitch. The second is navigational environment data, including wind speed, wind angle, sea water velocity, surface sea water velocity, and wave height. The internal navigation data are obtained by the onboard data acquisition center. The crew issue commands through the onboard centralized control system, while both the commands and the navigation status of the vessel are captured by the onboard data acquisition system. These data would be subsequently stored in the onboard data acquisition center and transmitted to the shore-based data information platform via satellite for further analysis and monitoring. The external navigation data are observed with the Global Positioning System (GPS). By combining this geolocation data with temporal information, we can match the environmental variables from external ocean datasets.

As for the external ocean datasets, they are provided by the Copernicus Marine Environment Monitoring Service (CMEMS), including three large datasets: Global Ocean Waves Analysis and Forecast dataset, Global Ocean Physics Analysis and Forecast dataset and Global Ocean Hourly Sea Surface Wind and Stress from Scatterometer and Model dataset. There are several small datasets in every large dataset. To ensure the accuracy of the navigational environment data, small datasets with the minimum spatial resolution (i.e., $0.083^\circ \times 0.083^\circ$) and temporal resolution (i.e., hourly) in the three large datasets were adopted to predict the energy consumption. Detailed information is provided in Table 2. The downloaded dataset is in NC format, which contains variables such as longitude, latitude, and time, with these dimensions covering the required meteorological data.

Table 2. Navigational environment data.

Dataset	Spatial Resolution	Temporal Resolution
Global Ocean Waves Analysis and Forecast	$0.083^\circ \times 0.083^\circ$	3 h
Global Ocean Physics Analysis and Forecast	$0.083^\circ \times 0.083^\circ$	1 h
Global Ocean Hourly Sea Surface Wind and Stress from Scatterometer and Model	$0.125^\circ \times 0.125^\circ$	1 h

In this paper, navigation data were derived from a voyage of this research vessel from 13 March 2024 to 19 March 2024. The navigation area of this voyage is shown in Figure 3. Navigational environment data of the navigation area in that period was downloaded from the CMEMS. It includes Sea surface wave maximum height (VCMX), sea surface wave from direction (VMDR), etc.

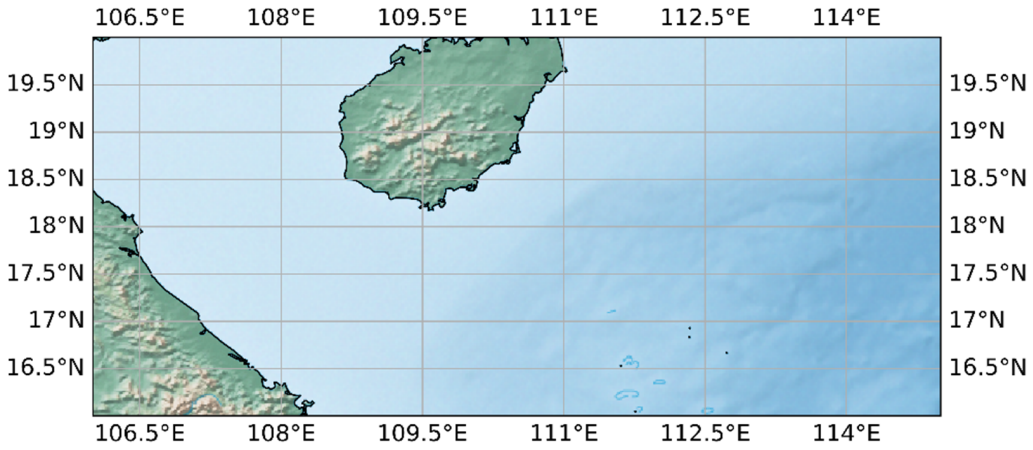
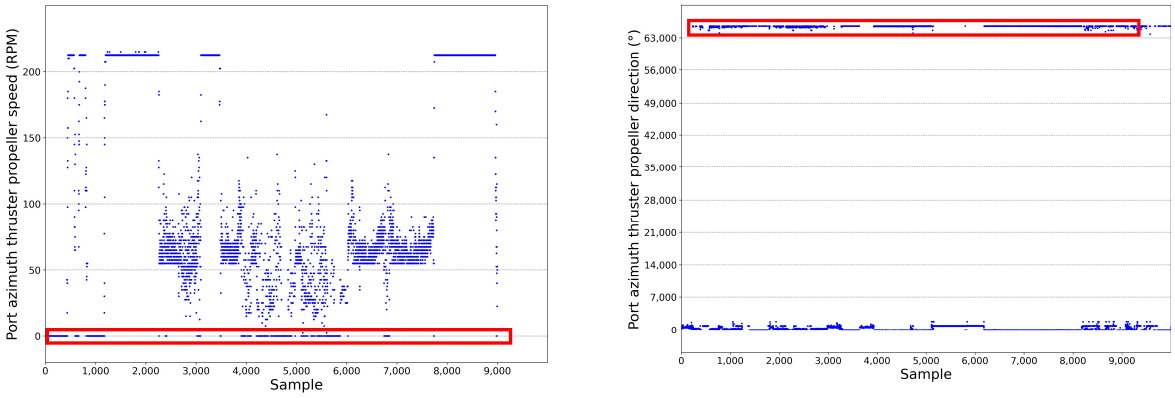


Figure 3. Navigation area.

3.2. Data Processing

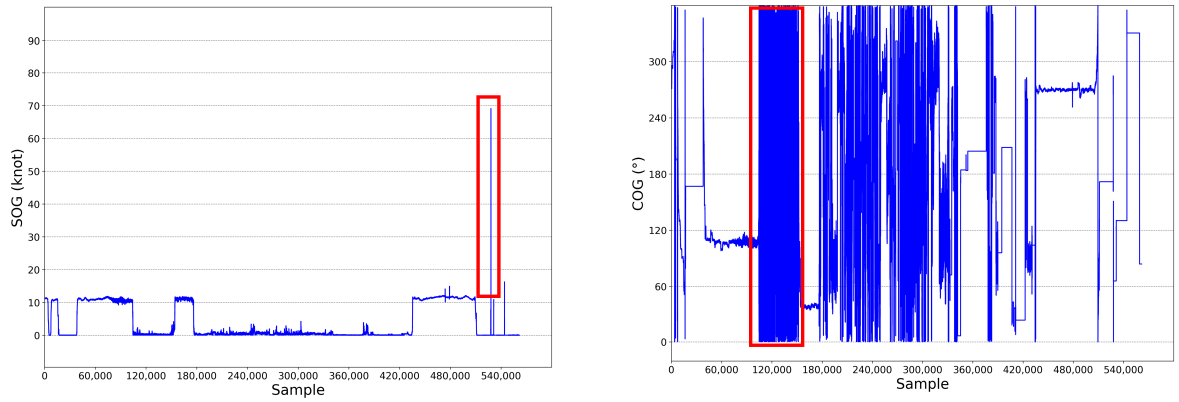
The navigation data were primarily obtained from different types of sensors. However, due to factors such as ship swaying caused by sea winds and waves, data conversion distortion, transmission delay, or other reasons, the raw data may contain some errors, as shown in Figure 4. For instance, the normal range of the SOG is typically between 0 and 20 knots; however, the raw data contains some abnormal values exceeding 20 knots. As for COG, many data samples exhibit frequent fluctuations from 0 to 360 degrees, which are attributed to the ship swaying against the wind and ocean waves. These errors and anomalies must be removed to ensure the accuracy of the prediction model.

The navigational environment data are characterized by significant temporal and spatial complexity, with considerable variations observed across different time and spatial regions. Since navigation data are collected through multiple sensors operating at different sampling frequencies. To synchronize the navigation data and navigational environment data in a tempo-spatial dimension, it is necessary to perform an initial time-scale alignment of the navigation data. Taking dataset A and dataset B as examples, in the first step of alignment, both datasets are sorted by their respective timestamps. Then, data points from datasets A and B with the closest timestamps are matched, allowing for a maximum time difference of several seconds between the two points. Following this initial alignment, the processed navigation data is further matched with the navigational environment data based on time, longitude, and latitude. In this step, the navigational environment data are selected by identifying the data points that are closest to the given conditions (time, latitude, and longitude).



(**a**) (**b**)

Figure 4. *Cont.*



(**c**) (**d**)

Figure 4. Anomalies and errors in raw navigation data: (**a**) Port azimuth thruster propeller speed with anomalies caused by ship docking and data transmission; (**b**) Port azimuth thruster propeller direction with data conversion distortions; (**c**) SOG with a slice of erroneous data; (**d**) COG with many anomalies caused by ship swaying.

3.3. Features Extraction

The propulsion system of this research vessel consists of four thrusters. The bow thruster facilitates lateral maneuvering at the bow, while the FWD azimuth thruster provides forward propulsion. The port azimuth thruster and STBD azimuth thruster are positioned on the left and right sides of the vessel, respectively, enhancing maneuverability in confined waterways. Together, these thrusters ensure the normal navigation of the research vessel while significantly improving the vessel's agility.

During voyages, ships experience wind and water resistance, and real-time fuel consumption would be influenced by a variety of internal and external factors. Many of these factors may exhibit strong interrelationships, resulting from complex physical processes. The tempo-spatial distribution characteristics of wind data in the navigation area are shown in Figure 5. It is evident that the wind speed exhibits significant variation across this navigation area.

To further investigate the interrelationships among these factors and simplify the input to the prediction model, the Pearson correlation coefficient matrix was selected as the evaluation criterion for these factors. The formula for the Pearson correlation coefficient is shown as follows:

$$\rho(x,y) = \frac{\sum_{i=1}^{n}(x_i-\overline{x})(y_i-\overline{y})}{\sqrt{\sum_{i=1}^{n}(x_i-\overline{x})^2\sum_{i=1}^{n}(y_i-\overline{y})^2}} \quad (4)$$

where x and y represent different feature variables, $\overline{x}$ and $\overline{y}$ denote the mean values of features x and y, respectively. The correlation coefficient ρ, measures the strength and direction of the linear relationship between features x and y. The resulting Pearson correlation coefficient matrix is shown in Figure 6.

From the Pearson correlation matrix, it is evident that correlation coefficients of the port azimuth thruster propeller speed (PATPS), STBD azimuth thruster propeller speed (SATPS), and SOG with fuel consumption (FC) are significantly higher than those of other features, indicating that these factors exhibit the strongest correlation with FC. During voyages, FWD azimuth thruster and bow thruster are rarely utilized, so the correlation coefficients of bow thruster propeller pitch (BTPP), FWD azimuth thruster propeller pitch (FATPP), and STBD azimuth thruster propeller direction (SATPD) with FC are relatively small. Furthermore, some feature variables exhibit strong correlations with each other, such as northward sea water velocity (VO) and surface sea water y velocity (VT). To prevent

overfitting during the prediction model training, certain correlated features were eliminated. The detailed selection and elimination of feature variables are shown in Table 3.

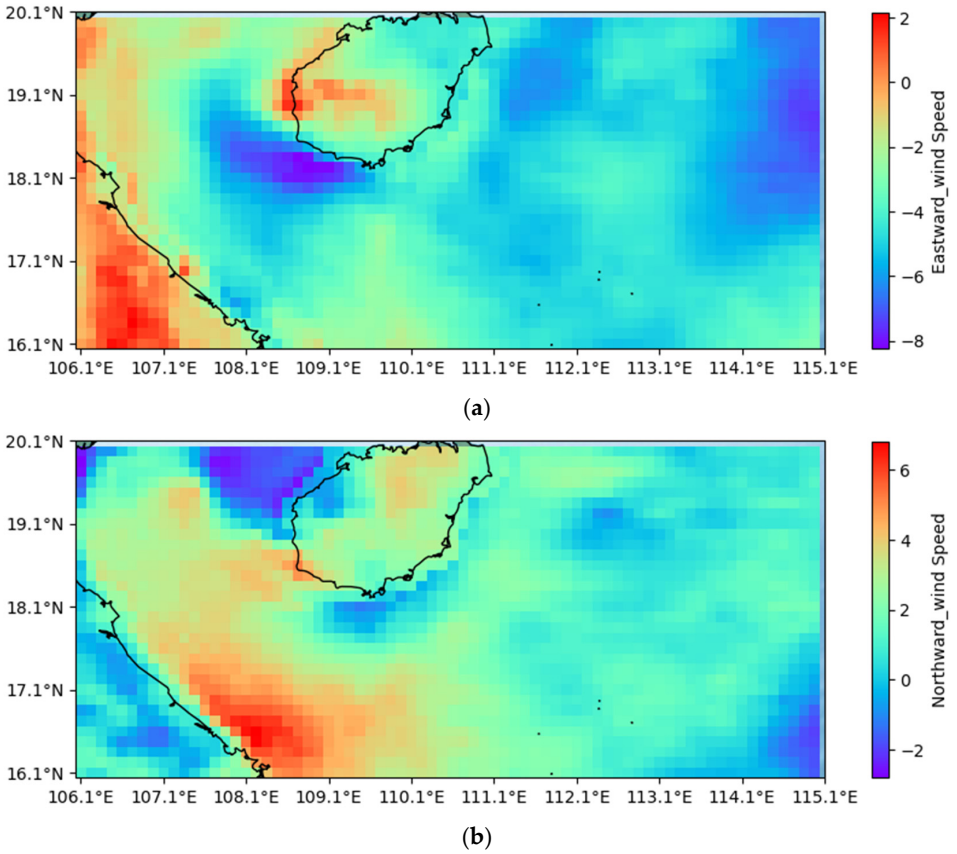


Figure 5. The spatial and temporal distribution characteristics of wind data in the navigation area: (**a**) Eastward wind data in 2024-03-14T03:00:00; (**b**) Northward wind data in 2024-03-14T03:00:00.

Table 3. Selection of feature variables.

Feature Variables	Abbreviation	
Bow thruster propeller pitch	BTPP	Selected
Port azimuth thruster propeller direction	PATPD	Selected
Port azimuth thruster propeller speed	PATPS	Selected
FWD azimuth thruster propeller pitch	FATPP	Selected
FWD azimuth thruster propeller direction	FATPD	Selected
STBD azimuth thruster propeller direction	SATPD	Selected
STBD azimuth thruster propeller speed	SATPS	Selected
Speed over ground	SOG	Selected
Course over ground	COG	Selected
Eastward wind speed	EWS	Selected
Northward wind speed	NWS	Selected
Eastward sea water velocity	UO	Selected
Northward sea water velocity	VO	Selected
Surface sea water x velocity	UT	Eliminated
Surface sea water y velocity	VT	Eliminated
Surface sea water x velocity due to tide	UTD	Eliminated
Surface sea water y velocity due to tide	VTD	Eliminated
Sea surface wave maximum height	VCMX	Eliminated
Sea surface wave significant height	VHM0	Selected
Sea surface wave from direction	VMDR	Selected

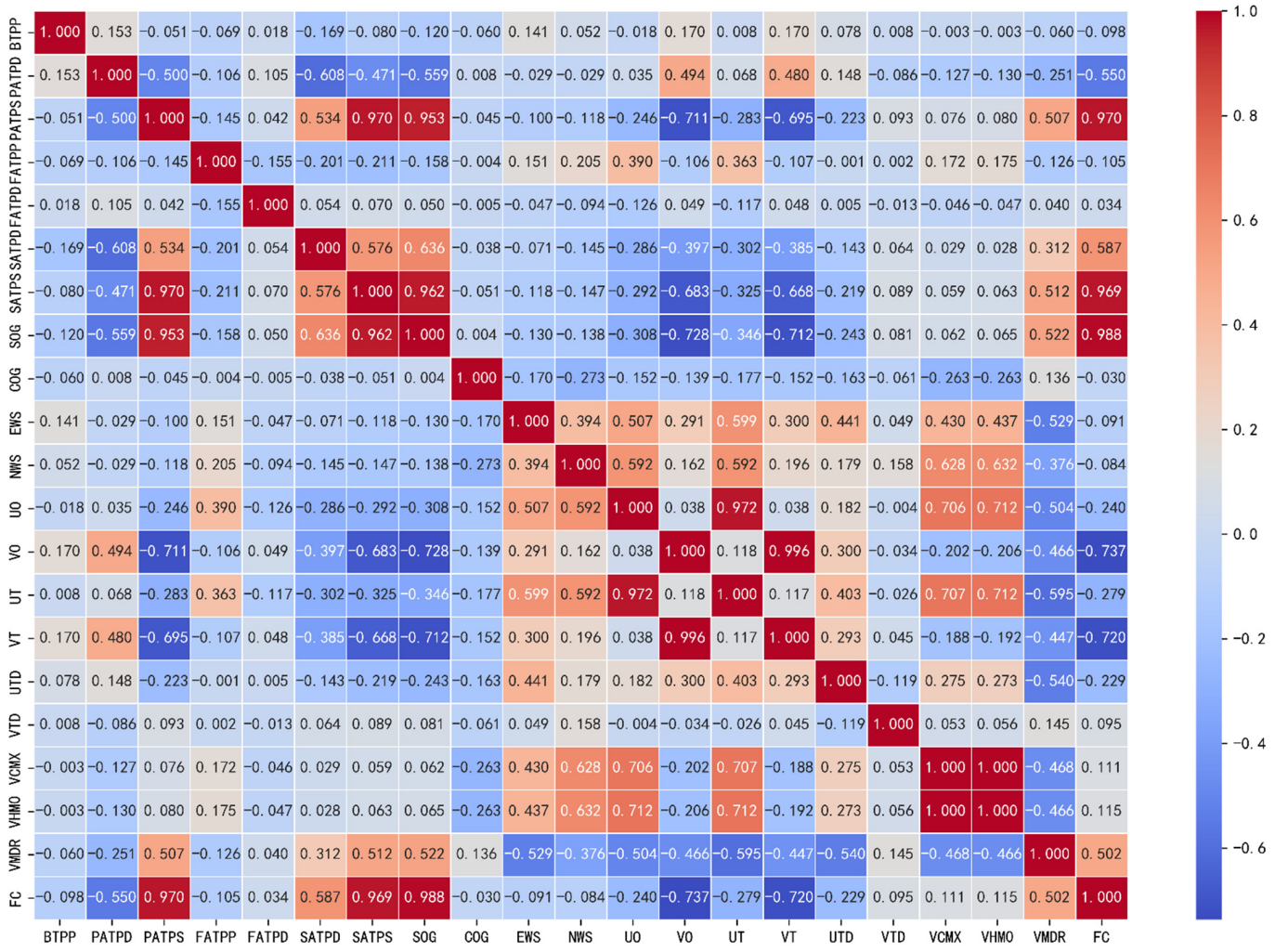


Figure 6. Pearson correlation coefficient analysis.

Furthermore, the actual wind speed, wind angle, sea water speed and sea water angle are calculated based on COG and their corresponding feature variables. For instance, the actual wind angle and wind speed are derived from the EWS, NWS, and COG. Ultimately, the remaining fifteen feature variables are selected as the input features of the prediction model, including nine navigation-related feature variables (BTPP, PATPD, PATPS, FATPP, FATPD, SATPD, SATPS, SOG, and COG) and six environmental feature variables (wind speed, wind angle, sea water speed, sea water angle, VHM0, and VMDR). A portion of the valid input data is presented in Table 4.

Table 4. Part of the valid input data.

PATPD /(°)	PATPS /(rpm)	SATPD /(°)	SATPS /(rpm)	SOG (m/s)	COG /(°)	VHM0 /(m)	...
59.167	62.5	−50.167	0.0	4.433	190.3	1.57	...
61.389	80	−50.167	0.0	4.433	151.1	1.57	...
87.278	67.5	−50.167	0.0	4.433	303.1	1.57	...
...	...	...	...	...	...	...	...
48.889	55.0	−41.667	57.5	0.027	204.4	0.86	...
49.444	55.0	−45.833	62.5	0.044	204.4	0.86	...
48.944	55.0	−44.444	60.0	0.014	204.4	0.86	...
...	...	...	...	...	...	...	...

4. Establishment and Evaluation of Prediction Model

4.1. DenseNet-Based Prediction Model Establishment

During voyages, various internal and external factors arising from complex navigation conditions can lead to dynamic changes in ship energy consumption. A high-accuracy energy consumption prediction model is essential for optimizing vessel operations, route planning, and fuel usage strategies. The proposed research framework is illustrated in Figure 7, and the steps for establishing the DenseNet-based prediction model are outlined as follows:

1. Data acquisition and processing. Collect and process both navigation data and navigational environment data for specific voyages, eliminating errors and anomalies, and synchronizing these data in the tempo-spatial dimension.
2. Data normalization and feature extraction. Based on the tempo-spatial distribution characteristics and the Pearson correlation coefficient matrix, select relevant feature variables to serve as input for the model.
3. Dataset partitioning and prediction model training. The input data will undergo overlap sampling and randomly divided into training and testing sets. Subsequently, the DenseNet-based prediction model is trained according to the processed data and the extracted feature variables.
4. Energy consumption prediction and analysis. The prediction results from the DenseNet-based prediction model will be analyzed by calculating settled performance metrics and compared with the results obtained from other deep learning models.

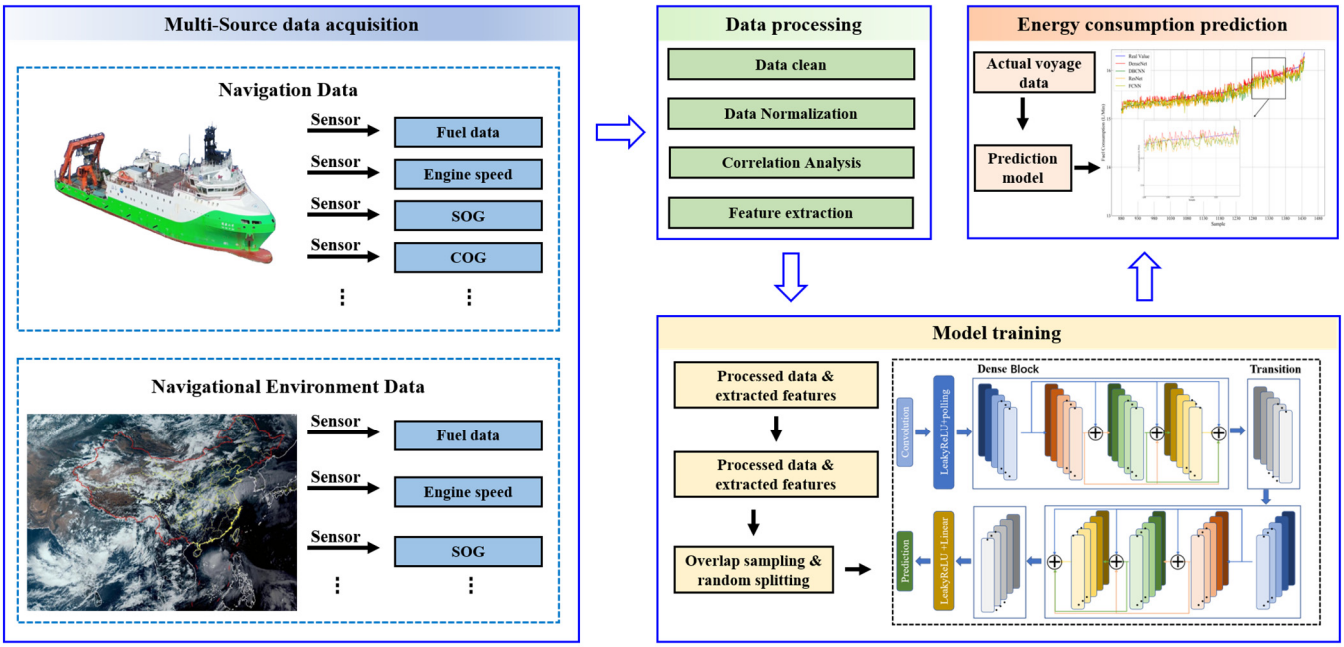


Figure 7. The framework of the DenseNet-based prediction model.

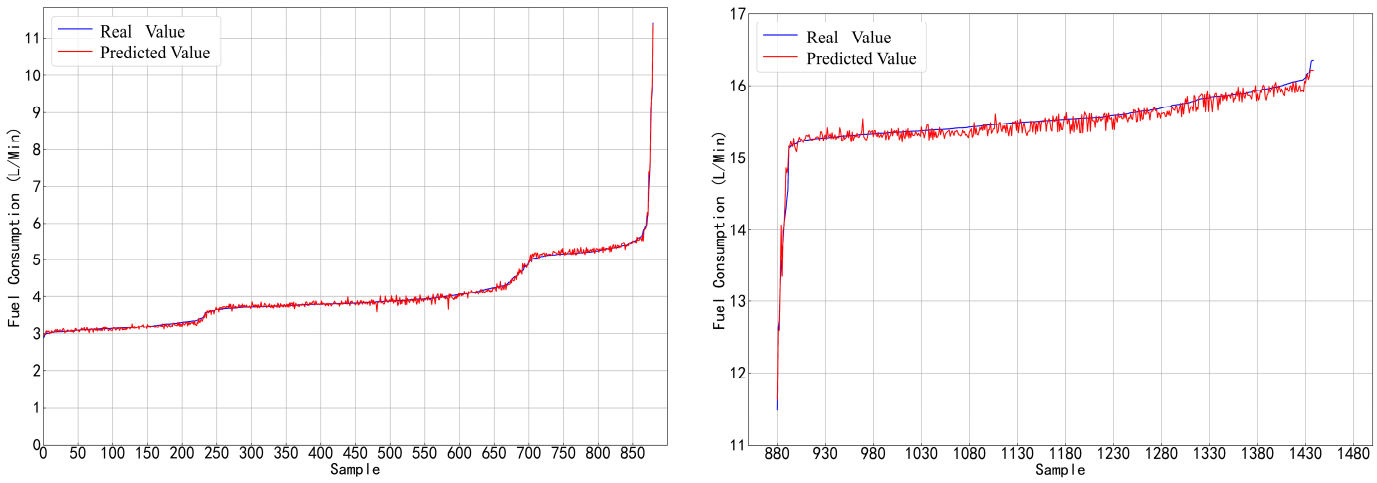
4.2. Validation of the Prediction Model

Based on the processed data and extracted feature variables, the DenseNet-based prediction model was developed on a desktop computer equipped with a 12th Gen Intel(R) Core(TM) i5-12490F CPU and 16 GB of main memory, running a 64-bit Windows 10 operating system. The model was implemented in Python 3.7, using the PyCharm Community Edition 2023.2.1 integrated development environment and the open-source deep learning framework PyTorch 2.1.0.

After data processing and feature extraction, a total of 7210 valid data samples were obtained. These samples would undergo normalization and overlap sampling, and they were then randomly split into two sets: 80% for training and the remaining 20% for testing. This process was repeated twice to generate two separate cases. To enhance training stability and convergence, a StepLR learning rate scheduler was employed. This schedule reduces the learning rate by a factor of gamma every specified number of epochs (step_size). This approach helps prevent overshooting by gradually lowering the learning rate as training progresses, encouraging the model to converge to an optimal solution. The parameters of the DenseNet-based prediction model are detailed in Table 5, and the prediction results are displayed in Figures 8–11.

Table 5. Parameters of the DenseNet-based prediction model.

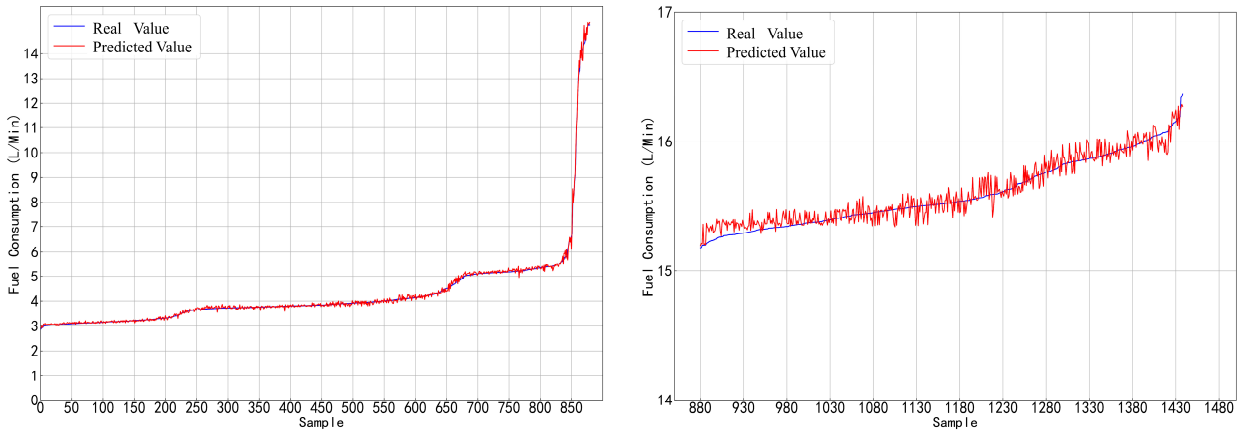
Parameters	Values
Epoch	250
Optimizer	Adam
Batch_size	64
Initial_learning_rate	0.001
Num_win	20
Stride	1
Step_size	80
Gamma	0.8



(**a**) (**b**)

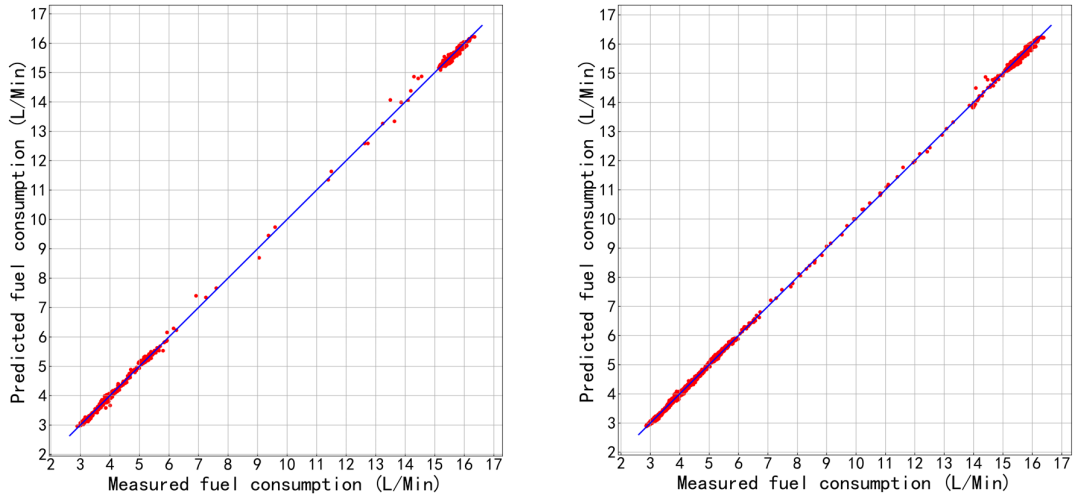
Figure 8. Prediction results of the DenseNet-based model (Case 1): (**a**) Segment A; (**b**) Segment B.

For clarity and presentation, the prediction results were reordered by the numerical value of each sample and divided into two segments, labeled A and B. Segment A shows the results for the first 880 samples after sorting, while Segment B includes the results of remaining samples. The results indicate that the DenseNet-based prediction model achieves high accuracy in forecasting ship energy consumption, with predicted values closely aligning with actual fuel consumption across diverse samples. This strong alignment proves the capability of DenseNet-based prediction model to capture the underlying patterns in fuel consumption effectively, even amidst fluctuations due to varying navigation and environmental conditions. Therefore, the DenseNet-based prediction model shows significant promise for enhancing predictive accuracy in complex navigation scenarios, suggesting its potential for optimizing operational strategies.



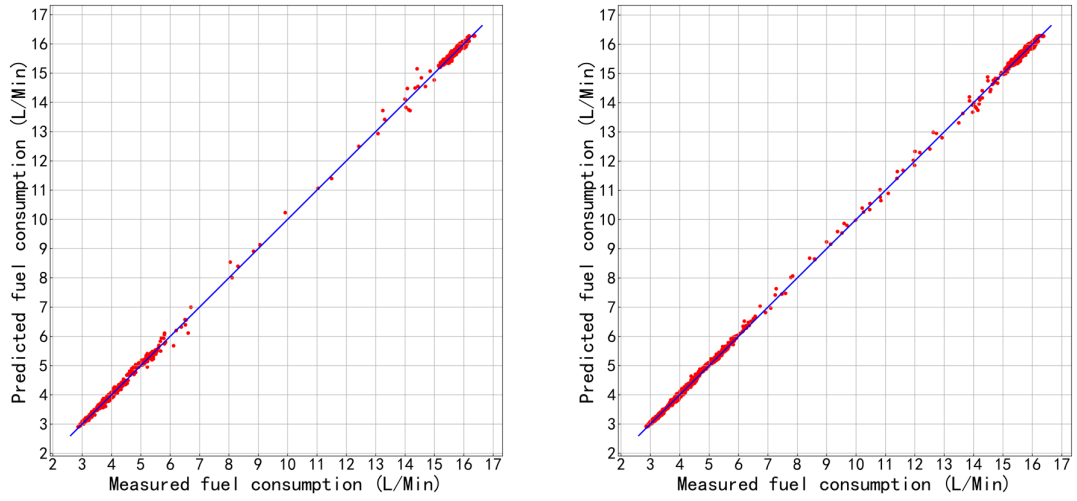
(**a**) (**b**)

Figure 9. Prediction results of the DenseNet-based model (Case 2): (**a**) Segment A; (**b**) Segment B.



(**a**) (**b**)

Figure 10. Scatterplot of the distribution of measured data and predicted results (Case 1): (**a**) Testing data; (**b**) Training data.



(**a**) (**b**)

Figure 11. Scatterplot of the distribution of measured data and predicted results (Case 2): (**a**) Testing data; (**b**) Training data.

4.3. Comparison of Different Prediction Model

To further evaluate the prediction performance of the proposed method, we conducted a comparative analysis with several traditional deep learning models, specifically DBCNN (Deep Batch-Normalization Convolutional Neural Network), ResNet (Residual Network), FCNN (Fully Connected Neural Network). Each model was trained and tested on the same training and testing sets to ensure consistency across comparisons. Additionally, several evaluation metrics were selected to provide a quantitative assessment of each model's predictive accuracy and overall performance. These metrics include Root Mean Squared Error (RMSE), Mean Absolute Error (MAE), Mean Squared Error (MSE), and the Coefficient of Determination (R^2). Together, these indicators offer a comprehensive evaluation, capturing different aspects of prediction accuracy and error distribution. The specific formulas for these metrics are outlined as follows:

$$MSE(x, \widetilde{x}) = \frac{1}{n}\sum_{i=1}^{n}(x_i - \widetilde{x_i})^2 \tag{5}$$

$$\mathrm{RMSE}(x, \widetilde{x}) = \sqrt{\frac{1}{n}\sum_{i=1}^{n}(x_i - \widetilde{x_i})^2} \tag{6}$$

$$R^2(x, \widetilde{x}) = 1 - \frac{\sum_{i=1}^{n}(x_i - \widetilde{x_i})^2}{\sum_{i=1}^{n}(x_i - \overline{x_i})^2} \tag{7}$$

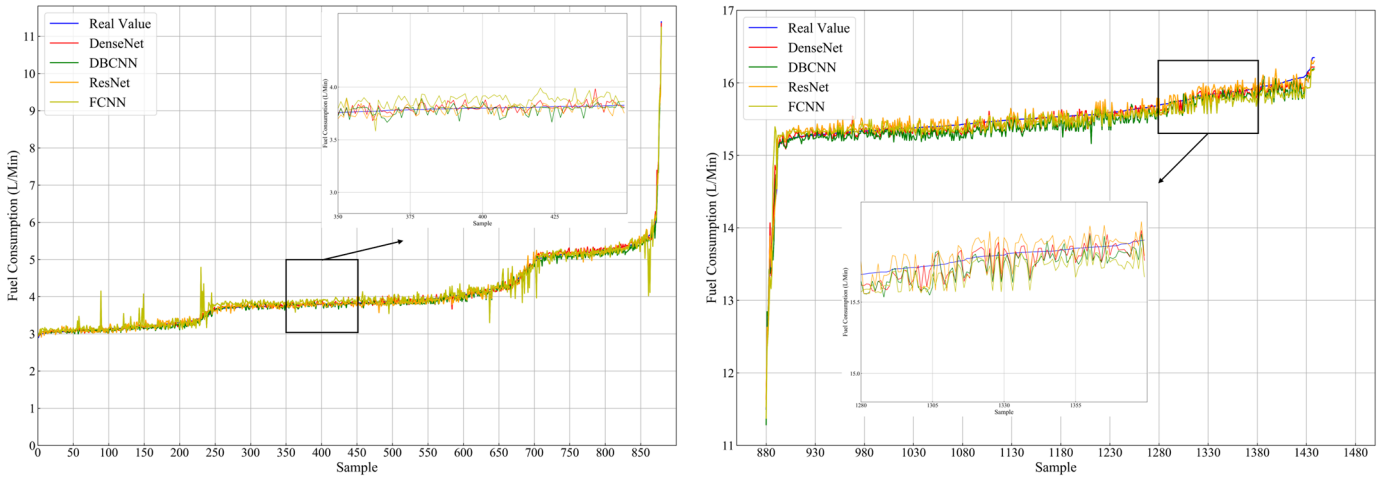
$$MAE(x, \widetilde{x}) = \frac{1}{n}\sum_{i=1}^{n}|x_i - \widetilde{x_i}| \tag{8}$$

where x_i, $\overline{x}$ indicate the real values and mean values, $\widetilde{x}$ represents the predicted values.

The prediction results for each energy consumption model are presented in Figures 12 and 13. The results of different evaluation metrics for the different models are detailed in Tables 6 and 7. It is evident that, compared to the DBCNN, ResNet, and FCNN prediction models, the DenseNet-based model exhibits the least fluctuation in predicted fuel consumption values, demonstrating strong consistency with the actual fuel consumption data. Furthermore, as shown in the performance comparison in Tables 6 and 7, the DenseNet-based model outperforms the DBCNN, ResNet, and FCNN models in both Case 1 and Case 2, achieving the lowest values for MSE, MAE, and RMSE, while attaining the highest R^2 values. While the performance differences between the DenseNet and ResNet models may appear relatively small in certain cases, we believe this is partly due to the limited dataset and the extensive data processing conducted in the earlier stages of the study. Nevertheless, even small improvements in accuracy and stability are significant in practical applications, as such gains contribute to more reliable and consistent predictions over time.

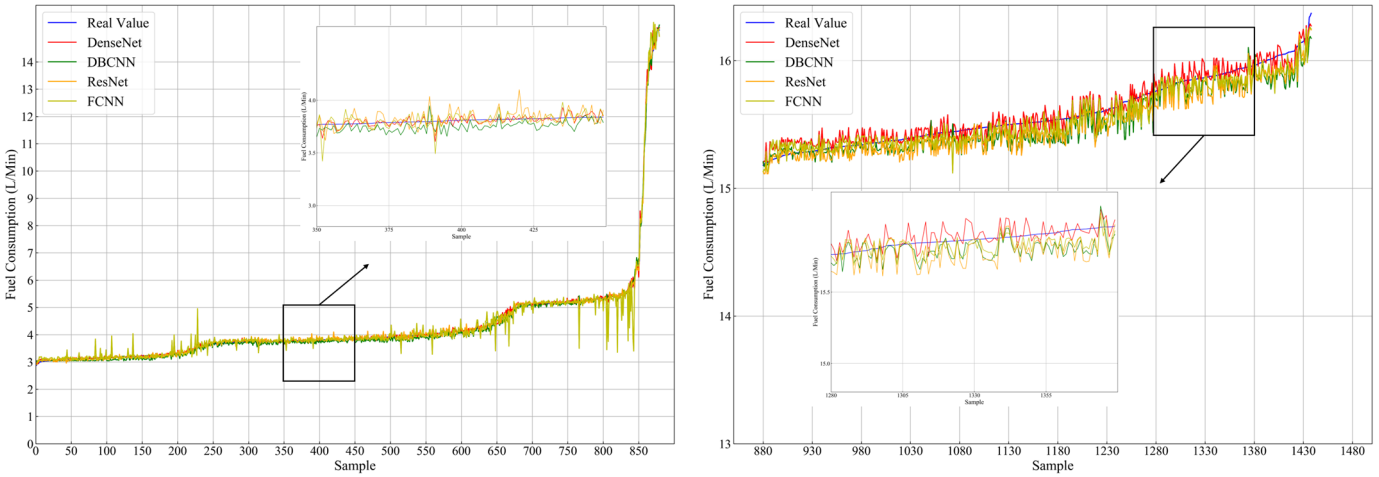
Table 6. The prediction performance of different models (Case 1).

Methods	RMSE	MAE	MSE	R^2
DenseNet	0.072385	0.051825	0.0052396	0.999836
DBCNN	0.097852	0.076525	0.0095750	0.999700
ResNet	0.082575	0.063328	0.00681868	0.999787
FCNN	0.152217	0.092271	0.0231699	0.999275



(**a**) (**b**)

Figure 12. Comparison of prediction results of different models (Case 1): (**a**) Segment A; (**b**) Segment B.



(**a**) (**b**)

Figure 13. Comparison of prediction results of different models (Case 2): (**a**) Segment A; (**b**) Segment B.

Table 7. The prediction performance of different models (Case 2).

Methods	RMSE	MAE	MSE	R^2
DenseNet	0.076548	0.052933	0.0058596	0.999818
DBCNN	0.104740	0.080561	0.0109705	0.999659
ResNet	0.088839	0.069309	0.0078925	0.999755
FCNN	0.204204	0.097049	0.0416994	0.998707

In conclusion, these results provide further evidence that the DenseNet-based prediction model outperforms the other models in terms of both accuracy and predictive reliability, reflecting its ability to effectively capture the underlying patterns in the dynamic and complex fluctuations of fuel consumption.

5. Conclusions

In this paper, a DenseNet-based prediction model is established to addresses the challenges of low accuracy and poor effectiveness in ship energy consumption prediction, caused by the diverse voyages and specialized operational missions of research vessels.

After the collection, analysis and features extraction of multi-source monitoring data, the processed data are utilized to establish the prediction model to achieve the energy consumption prediction of the research vessel. Based on the actual voyage data, the results demonstrate that the DenseNet-based prediction model effectively captures the complex feature associations in the data, leveraging complex feature information to achieving more accurate energy consumption prediction. Specifically, compared with DBCNN, ResNet and FCNN, the DenseNet-based prediction model exhibits better accuracy and stability, with a prediction error reduced to 0.051825. This indicates that the proposed method can provide practical implication for the improvement of ship energy efficiency and offers valuable guidance for energy conservation and emission reduction. By incorporating the sailing plans for future voyages (such as navigation areas, sailing speeds, etc.), we can apply the proposed model to predict fuel consumption for upcoming voyages and optimize voyage schedules accordingly.

Despite the promising results of the proposed approach, some limitations remain. Specifically, the prediction model is a black-box model, which requires a substantial amount of data and lacks interpretability. Furthermore, certain relevant variables, such as the ship's draft, trim, and shaft power, were not included in the current study due to the limitations of the available operational data. In future work, we aim to expand the dataset and validation scope, incorporating a more comprehensive set of feature variables. Additionally, we will explore techniques such as domain adaptation and transfer learning to improve the model's generalization ability and interpretability, and to compare its performance with other advanced methods. The goal is to enhance the model's applicability across various vessel types, operational scenarios, and environmental conditions.

Author Contributions: Conceptualization, G.T.; methodology, R.L.; formal analysis; investigation, X.L.; resources, H.M.; data curation, B.H.; writing—original draft preparation, G.T.; supervision, H.M. All authors have read and agreed to the published version of the manuscript.

Funding: This research received no external funding.

Data Availability Statement: The data will be made available upon request.

Conflicts of Interest: Author Bin Huang was employed by the company Hainan Moonsail Technology Co., Ltd. The remaining authors declare that the research was conducted in the absence of any commercial or financial relationships that could be construed as a potential conflict of interest.

References

1. Sirimanne, S.N.; Hoffman, J.; Juan, W.; Asariotis, R.; Assaf, M.; Ayala, G.; Benamara, H.; Chantrel, D.; Hoffmann, J.; Premti, A. Review of maritime transport 2019. In Proceedings of the United Nations Conference on Trade and Development, Geneva, Switzerland, 14–18 October 2019.
2. Fan, A.; Yang, J.; Yang, L.; Wu, D.; Vladimir, N. A review of ship fuel consumption models. *Ocean Eng.* **2022**, *264*, 112405. [CrossRef]
3. IMO. *Fourth Greenhouse Gas Study*; International Maritime Organization: London, UK, 2020.
4. Polakis, M.; Zachariadis, P.; de Kat, J.O. The energy efficiency design index (EEDI). In *Sustainable Shipping a Cross-Disciplinary View*; Springer Nature: London, UK, 2019; pp. 93–135.
5. Schaub, M.; Finger, G.; Riebe, T.; Dahms, F.; Hassel, E.; Baldauf, M. Data-based modelling of ship emissions and fuel oil consumption for transient engine operation. In Proceedings of the OCEANS 2019-Marseille, Marseille, France, 17–20 June 2019; pp. 1–5.
6. Wang, F. Intelligent transformation and upgrading of shipment industry: "force field analysis" and advancement strategies. *IET Conf. Proc.* **2024**, *2023*, 521–528. [CrossRef]
7. Wang, K.; Wang, J.; Huang, L.; Yuan, Y.; Wu, G.; Xing, H.; Wang, Z.; Wang, Z.; Jiang, X. A comprehensive review on the prediction of ship energy consumption and pollution gas emissions. *Ocean Eng.* **2022**, *266 Pt 2*, 112826. [CrossRef]
8. Nakamura, S.; Naito, S. Propulsive performance of a container ship in waves. *J. Soc. Nav. Archit. Jpn.* **1977**, *15*, 24–28.

9. Islam, H.; Soares, C.G. Effect of trim on container ship resistance at different ship speeds and drafts. *Ocean Eng.* **2019**, *183*, 106–115. [CrossRef]
10. Yang, L.; Chen, G.; Zhao, J.; Rytter, N.G.M. Ship speed optimization considering ocean currents to enhance environmental sustainability in maritime shipping. *Sustainability* **2020**, *12*, 3649. [CrossRef]
11. Lu, R.; Turan, O.; Boulougouris, E.; Banks, C.; Incecik, A. A semi-empirical ship operational performance prediction model for voyage optimization towards energy efficient shipping. *Ocean Eng.* **2015**, *110*, 18–28. [CrossRef]
12. Wang, K.; Xu, H.; Li, J.; Huang, L.; Ma, R.; Jiang, X.; Yuan, Y.; Mwero, N.A.; Sun, P.; Negenborn, R.R. A novel dynamical collaborative optimization method of ship energy consumption based on a spatial and temporal distribution analysis of voyage data. *Appl. Ocean Res.* **2021**, *112*, 102657. [CrossRef]
13. Liu, Y.; Wang, K.; Lu, Y.; Zhang, Y.; Li, Z.; Ma, R.; Huang, L. A Ship Energy Consumption Prediction Method Based on TGMA Model and Feature Selection. *J. Mar. Sci. Eng.* **2024**, *12*, 1098. [CrossRef]
14. Uyanik, T.; Yalman, Y.; Kalenderli, Ö.; Arslanoglu, Y.; Terriche, Y.; Su, C.L.; Guerrero, J.M. Data-Driven Approach for Estimating Power and Fuel Consumption of Ship: A Case of Container Vessel. *Mathematics* **2022**, *10*, 21. [CrossRef]
15. Yang, T.; Yang, Z.; Zhang, Y.; Yuan, C. Research Progress on Ship Speed Optimization for Energy Efficiency Improvement. *J. Navig. China* **2019**, *42*, 130–134.
16. Yan, R.; Wang, S.; Psaraftis, H.N. Data analytics for fuel consumption management in maritime transportation: Status and perspectives. *Transp. Res. Part E Logist. Transp. Rev.* **2021**, *155*, 102489. [CrossRef]
17. Liu, B.B.; Gao, D.J.; Yang, P.; Hu, Y.H. An Energy Efficiency Optimization Strategy of Hybrid Electric Ship Based on Working Condition Prediction. *J. Mar. Sci. Eng.* **2022**, *10*, 13. [CrossRef]
18. Zhou, J.; Zhao, Y.; Liang, J. Multiobjective route selection based on LASSO regression: When will the Suez Canal lose its importance? *Math. Probl. Eng.* **2021**, *2021*, 6613332. [CrossRef]
19. Işıklı, E.; Aydın, N.; Bilgili, L.; Toprak, A. Estimating fuel consumption in maritime transport. *J. Clean. Prod.* **2020**, *275*, 124142. [CrossRef]
20. Uyanık, T.; Karatuğ, Ç.; Arslanoğlu, Y. Machine learning approach to ship fuel consumption: A case of container vessel. *Transp. Res. Part D Transp. Environ.* **2020**, *84*, 102389. [CrossRef]
21. Hu, Z.; Zhou, T.; Zhen, R.; Jin, Y.; Li, X.; Osman, M.T. A two-step strategy for fuel consumption prediction and optimization of ocean-going ships. *Ocean Eng.* **2022**, *249*, 110904. [CrossRef]
22. Farag, Y.B.; Ölçer, A.I. The development of a ship performance model in varying operating conditions based on ANN and regression techniques. *Ocean Eng.* **2020**, *198*, 106972. [CrossRef]
23. Yuan, Z.; Liu, J.; Zhang, Q.; Liu, Y.; Yuan, Y.; Li, Z. Prediction and optimisation of fuel consumption for inland ships considering real-time status and environmental factors. *Ocean Eng.* **2021**, *221*, 108530. [CrossRef]
24. Chen, Y.; Sun, B.; Xie, X.; Li, X.; Li, Y.; Zhao, Y. Short-term forecasting for ship fuel consumption based on deep learning. *Ocean Eng.* **2024**, *301*, 117398. [CrossRef]
25. Sheng, D.; Meng, Q.; Li, Z.C. Optimal vessel speed and fleet size for industrial shipping services under the emission control area regulation. *Transp. Res. Part C Emerg. Technol.* **2019**, *105*, 37–53. [CrossRef]
26. Lv, Z.H.; Wang, N.N.; Lou, R.R.; Tian, Y.J.; Guizani, M. Towards carbon Neutrality: Prediction of wave energy based on improved GRU in Maritime transportation. *Appl. Energy* **2023**, *331*, 11. [CrossRef]
27. Kim, Y.R.; Jung, M.; Park, J.B. Development of a Fuel Consumption Prediction Model Based on Machine Learning Using Ship In-Service Data. *J. Mar. Sci. Eng.* **2021**, *9*, 25. [CrossRef]
28. Zheng, J.Q.; Zhang, H.R.; Yin, L.; Liang, Y.T.; Wang, B.H.; Li, Z.B.; Song, X.; Zhang, Y. A voyage with minimal fuel consumption for cruise ships. *J. Clean. Prod.* **2019**, *215*, 144–153. [CrossRef]
29. Chen, B.; Wang, X.; Wang, R.; Qiu, X.; Zhu, Z.; Ma, L. The Grey-box based Modeling Approach Research integrating Fusion Mechanism and Data. *J. Syst. Simul.* **2019**, *31*, 2575–2583.
30. Coraddu, A.; Oneto, L.; Baldi, F.; Anguita, D. Ship efficiency forecast based on sensors data collection: Improving numerical models through data analytics. In Proceedings of the OCEANS 2015—Genova, Genova, Italy, 18–21 May 2015; pp. 1–10.
31. Yang, L.; Chen, G.; Rytter, N.G.M.; Zhao, J.; Yang, D. A genetic algorithm-based grey-box model for ship fuel consumption prediction towards sustainable shipping. *Ann. Oper. Res.* **2019**. [CrossRef]
32. Coraddu, A.; Oneto, L.; Baldi, F.; Anguita, D. Vessels fuel consumption forecast and trim optimisation: A data analytics perspective. *Ocean Eng.* **2017**, *130*, 351–370. [CrossRef]
33. Xie, X.W.; Sun, B.Z.; Li, X.H.; Olsson, T.; Maleki, N.; Ahlgren, F. Fuel Consumption Prediction Models Based on Machine Learning and Mathematical Methods. *J. Mar. Sci. Eng.* **2023**, *11*, 19. [CrossRef]
34. Handayani, M.P.; Kim, H.; Lee, S.B.; Lee, J.H. Navigating Energy Efficiency: A Multifaceted Interpretability of Fuel Oil Consumption Prediction in Cargo Container Vessel Considering the Operational and Environmental Factors. *J. Mar. Sci. Eng.* **2023**, *11*, 26. [CrossRef]

35. Balcombe, P.; Brierley, J.; Lewis, C.; Skatvedt, L.; Speirs, J.; Hawkes, A.; Staffell, I. How to decarbonise international shipping: Options for fuels, technologies and policies. *Energy Convers. Manag.* **2019**, *182*, 72–88. [CrossRef]
36. Jiang, W.; Wu, G. Fore-Body Lines Design of Oceanographic Research Vessel. *Ship Eng.* **2021**, *43*, 1–5.
37. Ni, Q.; Li, S.; Ruan, W.; Hou, X.; Yang, L. Application of SBD technique on TAN SUO YI HAO' scientific investigation ship hullform design. *J. Ship Mech.* **2018**, *22*, 54–60.
38. Le, T.; Vo, M.T.; Vo, B.; Hwang, E.; Rho, S.; Baik, S.W. Improving electric energy consumption prediction using CNN and Bi-LSTM. *Appl. Sci.* **2019**, *9*, 4237. [CrossRef]
39. Zhang, W.; Li, X.; Ding, Q. Deep residual learning-based fault diagnosis method for rotating machinery. *ISA Trans.* **2019**, *95*, 295–305. [CrossRef] [PubMed]
40. He, K.; Zhang, X.; Ren, S.; Sun, J. Deep residual learning for image recognition. In Proceedings of the IEEE Conference on Computer Vision and Pattern Recognition, Las Vegas, NV, USA, 27–30 June 2016; pp. 770–778.
41. Yang, S.; Ling, L.; Li, X.; Han, J.; Tong, S. Industrial Battery State-of-Health Estimation with Incomplete Limited Data Toward Second-Life Applications. *J. Dyn. Monit. Diagn.* **2024**, *3*, 246–257. [CrossRef]
42. Li, X.; Zhang, C.; Li, X.; Zhang, W. Federated transfer learning in fault diagnosis under data privacy with target self-adaptation. *J. Manuf. Syst.* **2023**, *68*, 523–535. [CrossRef]
43. Zhao, L.; Chen, Y. Dynamics and Fault Diagnosis of Railway Vehicle Gearboxes: A Review. *J. Dyn. Monit. Diagn.* **2024**, *3*, 83–98. [CrossRef]
44. Li, X.; Yu, S.P.; Lei, Y.G.; Li, N.P.; Yang, B. Dynamic Vision-Based Machinery Fault Diagnosis with Cross-Modality Feature Alignment. *IEEE-CAA J. Autom. Sin.* **2024**, *11*, 2068–2081. [CrossRef]
45. Li, X.; Zhang, W.; Li, X.; Hao, H.S. Partial Domain Adaptation in Remaining Useful Life Prediction With Incomplete Target Data. *IEEE-ASME Trans. Mechatron.* **2024**, *29*, 1903–1913. [CrossRef]
46. Zhang, W.; Hao, H.; Zhang, Y. State of charge prediction of lithium-ion batteries for electric aircraft with swin transformer. *IEEE-CAA J. Autom. Sin.* **2024**, 1–3. [CrossRef]

Disclaimer/Publisher's Note: The statements, opinions and data contained in all publications are solely those of the individual author(s) and contributor(s) and not of MDPI and/or the editor(s). MDPI and/or the editor(s) disclaim responsibility for any injury to people or property resulting from any ideas, methods, instructions or products referred to in the content.